



## Implication of M2 macrophage on NLRP3 inflammasome signaling in mediating the neuroprotective effect of Canagliflozin against methotrexate-induced cognitive impairment

Lobna H. Khedr<sup>a</sup>, Rania M. Rahmo<sup>a</sup>, Omar M. Eldemerdash<sup>b</sup>, Engy M. Helmy<sup>c</sup>, Felopateer A. Ramzy<sup>c</sup>, George H. Lotfy<sup>c</sup>, Habiba A. Zakaria<sup>c</sup>, Marine M. Gad<sup>c</sup>, Marina M. Youhanna<sup>c</sup>, Manar H. Samaan<sup>c</sup>, Nevert W. Thabet<sup>c</sup>, Reem H. Ghazal<sup>c</sup>, Mostafa A. Rabie<sup>d,\*</sup>

<sup>a</sup> Department of Pharmacology and Toxicology, Faculty of Pharmacy, Misr International University (MIU), Cairo 44971, Egypt

<sup>b</sup> Department of Biochemistry, Faculty of Pharmacy, Misr International University (MIU), Cairo 44971, Egypt

<sup>c</sup> Pharmacy Senior Students, Faculty of Pharmacy, Misr International University (MIU), Cairo 44971, Egypt

<sup>d</sup> Department of Pharmacology and Toxicology, Faculty of Pharmacy, Cairo University, 11562 Cairo, Egypt

### ARTICLE INFO

#### Keywords:

Methotrexate  
Cognitive impairment  
NLRP3 inflammasome  
Microglial polarization  
Inflammasomes and neuroinflammation

### ABSTRACT

Methotrexate (MTX), a chemotherapeutic antimetabolite, has been linked to cognitive impairment in cancer patients. MTX-induced metabolic pathway disruption may result in decreased antioxidant activity and increased oxidative stress, influencing hippocampal neurogenesis and microglial activation. Nuclear factor-kappa B (NF-κB), an oxidative stress byproduct, has been linked to MTX toxicity via the activation of NLRP3 inflammasome signaling. Macrophage activation and polarization plays an important role in tissue injury. This differentiation may be mediated via either the Toll-like receptor 4 (TLR4) or NLRP3 inflammasome. Interestingly, Canagliflozin (CANA), a sodium-glucose cotransporter 2 (SGLT2) inhibitor has been recently reported to exert anti-inflammatory effects by modulating macrophage polarization balance. This study aimed to investigate CANA's protective effect against MTX-induced cognitive impairment, highlighting the possible involvement of TLR4/ NF-κB crosstalk with NLRP3 inflammasome activation and macrophage polarization. Forty-eight Male Wistar rats were divided into 4 groups; (1) received saline orally for 30 days and intravenously on days 8 and 15. (2) received Canagliflozin (CANA; 20 mg/kg/day; p.o.) for 30 days. (3) received MTX (75 mg/kg, i.v.) on day 8 and 15, then they were injected with four i.p. injections of leucovorin (LCV): the first dose was 6 mg/kg after 18 h, and the remaining doses were 3 mg/kg after 26, 42, and 50 h of MTX administration. (4) received MTX and LCV as in group 3 in addition to CANA as in group 2. MTX-treated rats showed cognitive deficits in spatial and learning memory as evidenced in the novel object recognition and Morris water maze tests. MTX exerted an oxidative effect which was evident by the increase in MDA and decline in SOD, GSH and GPx. Moreover, it exerted an inflammatory effect via elevated caspase-1, IL-1β and IL-8. CANA treatment restored cognitive ability, reduced MTX-induced oxidative stress and neuroinflammation via attenuation of TLR4/NF-κB/NLRP3 signaling, and rebalanced macrophage polarization by promoting the M2 phenotype. Hence, targeting molecular mechanisms manipulating macrophage polarization may offer novel neuroprotective strategies for preventing or treating MTX-induced immune modulation and its detrimental sequel.

### 1. Introduction

Methotrexate (MTX) is an antifolate chemotherapeutic drug that demonstrates efficacy against a wide range of cancer types [1]. The

utilization of MTX is currently on the rise as a result of the high incidence of cancer; yet it is widely recognized for its significant neurological adverse effects. Thus, MTX is widely recognized as a neurotoxic chemotherapeutic drug that is extensively utilized [2]. Although MTX is

\* Corresponding author at: Department of Pharmacology and Toxicology, Faculty of Pharmacy, Cairo University, Kasr El-Aini Str., 11562 Cairo, Egypt.  
E-mail address: [Mostafa.mohammed@pharma.cu.edu.eg](mailto:Mostafa.mohammed@pharma.cu.edu.eg) (M.A. Rabie).

generally believed to fail to cross the blood–brain barrier, it has been observed that high doses of MTX can have neurotoxic effects [3]. The cognitive impairment associated with this neurotoxicity is characterized by deficiencies in memory, decreased capacity for learning, difficulties in concentration, and impaired decision-making abilities [4]. Although the mechanism of MTX-induced neurotoxicity has not been extensively investigated, recent studies have proposed several ideas to explain this phenomenon. These hypotheses include decreased hippocampal neurogenesis, neuroinflammation, oxidative stress, and activation of apoptosis [5–7]. Hence, it is imperative to protect the cognitive abilities of individuals with cancer through the identification of novel molecular targets and therapies that mitigate the neurotoxic effects of MTX.

MTX-induced oxidative stress has been seen to elevate levels of reactive oxygen species (ROS), which then triggers cellular damage and the subsequent release of high mobility group box-1 (HMGB1) protein [8]. The HMGB1 protein is released into the extracellular space, where it functions as a molecule associated with damage, known as a damage-associated molecular pattern (DAMP). It interacts with the receptor called Toll-like receptor 4 (TLR4), which in turn triggers an inflammatory response [9,10]. Activation of TLR4 led to the recruitment of myeloid differentiation factor-88 adaptor protein (MyD88) which serves as an inflammatory adaptor protein downstream of TLR4 [11]. The MyD88 pathway has been established as a documented mechanism for inducing the production and translocation of the nuclear factor kappa-light-chain-enhancer of activated B cells (NF- $\kappa$ B), hence initiating the transcription of proteins that contribute to the formation of inflammasomes [11,12].

Among NF- $\kappa$ B p65 expressed proteins is the nucleotide-binding domain, leucine-rich-containing family, pyrin domain-containing-3 (NLRP3). The NLRP3 inflammasome is then assembled as a result of NLRP3's subsequent binding to the pro-caspase 1 via the adaptor protein (ASC) [13,14]. Inflammasomes are intricate assemblies consisting of several proteins that enhance the generation of proinflammatory mediators [15]. The NLRP3 inflammasome in a rat model of MTX-induced kidney injury has been observed to exhibit a significant rise when exposed to ROS-activated NF- $\kappa$ B p65 [16]. Furthermore, NF- $\kappa$ B plays a crucial role in the activation of pro-IL-1 $\beta$  and pro-IL-18, in addition to its involvement in the upregulation of NLRP3 expression [17]. The NLRP3 protein cleaves the pro-caspase1 molecule, resulting in the formation of active caspase 1. This process is crucial for the activation of pro-IL-1 $\beta$  and pro-IL-18, leading to the production of IL-1 $\beta$  and IL-18, respectively [18,19]. Therefore, the inflammasome assumes an essential position in the inflammatory response across different models by facilitating the generation of inflammatory cytokines and promoting pyroptosis, a form of programmed cell death associated with inflammation [20].

In recent studies, the involvement of microglia-associated pyroptosis has been documented in the inflammatory processes observed in several central nervous system (CNS) models, including multiple sclerosis, Alzheimer's disease, traumatic brain injury, and other neurodegenerative disorders [21–23]. Microglia, a prominent type of immune cell, is known to be activated and assumes a critical function in the process of neuroinflammation [24]. Microglia has a pair of different phenotypes, namely M1 and M2. The M1 phenotype is characterized by the production of pro-inflammatory mediators, which in turn promote inflammatory responses. Conversely, the M2 phenotype is associated with anti-inflammatory properties and is known to mediate neuroprotective benefits [25]. The activation of NF- $\kappa$ B and NLRP3 inflammasome has been observed to stimulate the M1 microglia phenotype while inhibiting the M2 microglia phenotype, hence leading to the induction of neuroinflammation [26]. The TLR4/MyD88/ NF- $\kappa$ B/NLRP3 inflammasome pathway has been extensively investigated in many CNS and renal models. However, its involvement in MTX-induced neurotoxicity has not been thoroughly examined. Therefore, the objective of this study is to investigate the impact of MTX on this particular pathway and its influence on microglial polarization.

Considering the escalating and imperative utilization of MTX in the

management of diverse malignancies and medical conditions, there arises a necessity to identify a concurrent therapeutic approach that possibly mitigate its adverse neurological effects. Hence, Canagliflozin (CANA) emerged as a potential mitigator for these adverse effects. CANA, a sodium-glucose cotransporter 2 (SGLT2) inhibitor, has recently been proven to possess notable anti-inflammatory properties [27]. The efficacy of CANA in mitigating LPS-induced acute lung injury has been demonstrated by its ability to reduce the activation of NF- $\kappa$ B, hence influencing the polarization of microglia. This leads to a favorable shift towards the activation of M2 microglia and inhibition of the M1 phenotype [28]. CANA further showed potency in having a hepatoprotective impact by reducing oxidative stress indicators and effectively lowering the expression level of TLR4 [29]. A recent study reported that the administration of CANA effectively suppresses the activation of the NLRP3 inflammasome, leading to a notable reduction in the levels of IL-1 $\beta$  and IL-18. This finding implies that CANA holds potential benefits for diabetic patients who have been diagnosed with pneumonia [30]. The aforementioned evidence suggests that CANA holds promise as a potential co-treatment with MTX to mitigate its neurotoxic effects. This study aims to conduct a comparative analysis between the impact of MTX alone and the combined impact of MTX with CANA on the molecular pathway TLR4/MyD88/NF- $\kappa$ B/NLRP3 inflammasome. Furthermore, the study investigates the effects of these interventions on microglial activation and neuroinflammation.

## 2. Materials and methods

### 2.1. Experimental animals

Forty-eight male Wistar rats, weighing 160–200 g, were obtained from the animal facility of Egyptian Drug Authority (EDA, Giza, Egypt) and kept in the animal facility (Misr International University, Cairo, Egypt) under a constant temperature ( $25 \pm 2^\circ\text{C}$ ), humidity ( $60 \pm 10\%$ ), and a 12/12 h light/dark cycle. Prior to experimentation, animals were allowed to acclimatize for 7 days. Rats were housed as 4 rats per polycarbonate rat cage (430x290x201mm) and during the entire period, animals had unrestricted access to water and chow pellets.

### 2.2. Ethical statement

The investigational protocol was approved by Research Ethics Committee, Faculty of Pharmacy, Cairo University, Cairo, Egypt (Permit Number 3331) that was implemented in accordance with Health Guide for Care and Use of Laboratory Animals (No. 85–23, revised 2011). All efforts were carried out to lessen animal suffering.

### 2.3. Drugs and chemicals

Methotrexate (MTX; 50 mg/vial; Methotrexate®; Mylan S.A.S., France) and Leucovorin (LCV; 50 mg/vial; Calcifolinon®; Global Napi, Egypt) were administrated intravenously, whereas Canagliflozin (CANA; 100 mg/tablet; Invokana®; Janssen, Italy) was dissolved in saline and administrated orally.

### 2.4. Experimental design

Rats were randomly given numbers and then allocated to the four groups ( $n = 12/\text{group}$ ) according to randomization table generated by random.org and classified as follows: Group 1 received saline orally for 30 days and intravenously on days 8 and 15. Group 2 received Canagliflozin (CANA; 20 mg/kg/day; p.o.) dissolved in 0.9 % saline for 30 days [31–33]. Group 3 and 4 received MTX (75 mg/kg, i.v. in one of the two lateral tail veins) on day 8 and 15 [5,34], then they were injected with four i.p. injections of LCV: the first dose was 6 mg/kg, i.p. after 18 h, and the remaining doses were 3 mg/kg, i.p. after 26, 42, and 50 h of MTX administration [35,36], whereas group 3 left untreated to be

nominated as MTX-group, meanwhile group 4 was treated with CANA (20 mg/kg/day; p.o.) to be designed as MTX/CANA group. The study was conducted for 30 days as illustrated in [Fig. 1].

## 2.5. Bioinformatic analysis

Pathway Studio® (Elsevier, Netherlands, accessed: September 24, 2022) (<https://www.pathwaystudio.com>), a publicly available platform, was used to investigate the potential interactions between MTX, CANA, and apoptosis process. We included TLR4, MyD88, NF-κB, NLRP3 and inflammasome in our study since they are known to be involved in inflammasome and apoptosis process.

## 2.6. Behavioral analysis

After 24-hrs. of the last dose of CANA administration, animals were subjected to behavioral analysis to assess their cognitive and memory impairments using novel object recognition (NOR) and Morris water maze (MWM) tests with 2 hrs. lag between the tests.

### 2.6.1. Novel object recognition (NOR) test

The NOR test was carried out to assess the recognition memory of the rat to recall the old object and to identify the newer one [37,38]. The apparatus comprised of a wooden box (1 m x 1 m x 0.5 m) with blue cubes (familiar object) and green cylinder (novel object) and the test was completed over 3 consecutive days; habituation day, training day and testing day. In the habituation day, rats were left for 10 min to explore the arena without any items, whereas on the training day, rats were placed in the box for 10 min also, but with 2 blue identical cubes present on the opposite corners of the arena for investigation. On the third (test) day, one of the blue cubes was replaced with green cylinder and the rats were left for 3 min to explore the objects. Between each trial, the arena, and the items were cleansed with 70 % alcohol to eliminate any odor interference. To assess cognitive function, preference index (PI) was determined as time spent by the rat investigating the novel object divided by total time of exploration, along with discrimination index (DI) that was calculated as difference in time between examining familiar and novel objects divided by total time of exploration, using ANY-maze (version 7.1, Stoelting Co, IL, USA) [36].

### 2.6.2. Morris water maze (MWM) test

The MWM test was performed to evaluate the spatial learning and memory retention of the rats [8], using a circular pool with dimension

(diameter 150 cm and height 60 cm) that was divided into 4 identical quadrants. Each rat was subjected to 4 training sessions per day for 3 consecutive days to receive a total of 12 training sessions prior to probe test on the fourth day [39]. During the training (acquisition) phase, the platform was placed in the target quadrant and the rat was left freely for 60 sec to reach the platform and if the rat did not reach the latter, he was directed to it and left for 10 sec. In the probe test, the platform was removed, and the rats were left for 60 sec to investigate the pool. The latency to reach target quadrant, and time spent in the target quadrant as well as path efficacy was calculated using analyzed using ANY-maze (version 7.1, Stoelting Co, IL, USA) [7].

## 2.7. Hippocampal processing

After behavioral analysis completion, animals were euthanized by cervical dislocation under thiopental anesthesia (50 mg/kg; i.p.). The brains were dissected directly, rinsed with ice-cold saline, and divided into 3 subsets. In the first and second subset, the hippocampi was separated from the brain and snap frozen in liquid nitrogen and stored at  $-80^{\circ}\text{C}$ . Indeed, the 1st subset ( $n = 6/\text{group}$ ) was used for enzyme-linked immunosorbent assay (ELISA) assessment after homogenization in phosphate buffer saline (PBS, pH = 7.4), whereas the 2nd subset ( $n = 3/\text{group}$ ) was immersed in RIPA buffer provided with phosphatase and protease inhibitors for western blot analysis. Finally, the last subset (whole brain;  $n = 3/\text{group}$ ) was fixed into 10 % buffered formalin saline for histological examination and immunohistochemical analysis of CD86 and CD163 in hippocampal Cornu Ammonis 3 (CA3) region.

### 2.7.1. Enzyme-Linked immunosorbent assay (ELISA)

Rat MyBioSource ELISA kits were procured to assess IL-18 (cat#: MBS260091), IL-1β ((cat#: MBS825017), tumor necrosis factor-α (TNF-α; cat#: MBS2507393), transforming growth factor beta (TGF-β; cat#: MBS260302), inducible nitric oxide synthase (iNOS; cat#: MBS263618) and arginase 1 (cat#: MBS917512), whereas ELISA kit purchased from LSBio (WA, USA) was used to determine HMGB1 (cat#: LS-F4039). In parallel, malondialdehyde (MDA; cat#: MD 2529), reduced glutathione (GSH; cat#: GR 2511), superoxide dismutase (SOD; cat#: SD 2521), and glutathione peroxidase (GPx; cat#: GP 2524) were evaluated colorimetry using commercial kits purchased from Biodiagnostic (Giza, EG). All the procedure were carried out in accordance with the manufacturers' protocol and these parameters were normalized to protein content evaluated via Bradford assay [40].

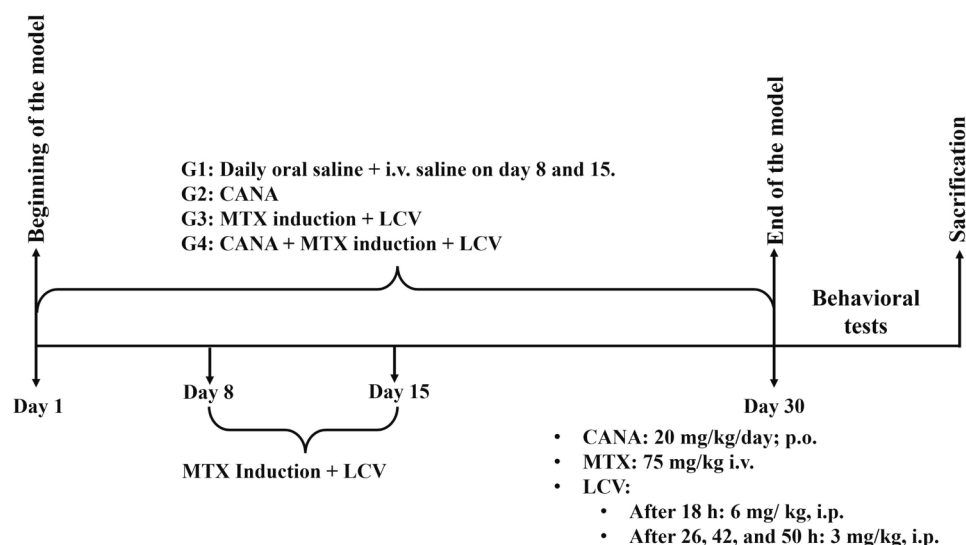


Fig. 1. Experimental model timeline.

### 2.7.2. Western blotting analysis

Hippocampal TLR4, NLRp3, ASC1, Caspase, and Procaspase as well as total and phosphorylated NFκB p65 (pS536-NFκB p65) were evaluated using western blot analysis. Bradford assay was used to measure the protein concentration in each sample, where 20 µg protein were loaded and separated via SDS-PAGE, then transferred to PVDF membrane and blocked with tris-buffered saline with Tween 20 (TBST) and 3 % bovine serum albumin for 1 hr. Subsequently, the membrane was incubated with either anti-TLR4 (1:100; cat# 48-2300), anti-NLRP3 (0.2 µg/mL; cat# 48-2300), anti-ASC1 (1:1000; cat# PA5-90403), anti-caspase (1:300; cat# BSM-33199 M), anti-procaspase (2 µg/mL; cat# MA1-91637), anti-total NFκBp65 (5 µg/mL; cat# PA5-16545), anti-pS536-NFκB p65 (1:1000; cat# MA5-15181) or anti-β-actin (1:5000; cat# MA1-140) primary antibodies (ThermoFisher Scientific, MA, USA) at 4 °C on a roller shaker overnight. Later, membranes were rinsed with TBST and incubated with HRP-conjugated goat anti-rabbit immunoglobulin (1:1000; Dianova, HH, Germany) for 1 hr at room temperature. Finally, the blots were detected with enhanced chemiluminescence reagents (Amersham Biosciences, NJ, USA) and the protein was quantified by densitometric analysis using a scanning laser densitometer (GS-800 system, Bio-Rad, CA, USA). The results are presented as arbitrary units (AU) after normalization for β-actin protein expression.

### 2.8. Histology and immunohistochemistry

Brain sample (n = 3) were immersed immediately in 10 % buffered-formalin saline for 72 hrs. and processed for paraffin-embedded blocks preparation. Brain sections (4 µm) were trimmed and stained with hematoxylin and eosin (H&E) for evaluation CA3 hippocampal area. All procedure of fixation and staining were carried out according to the Handbook of Histopathological and Histochemical Techniques [41].

Immunohistochemical assessments were implemented using deparaffinized sections (5 µm) that were trimmed for the investigation of hippocampal CD86 and CD163 in CA3 region. The sections were blocked with 3 % H<sub>2</sub>O<sub>2</sub> for 15 min, then incubated with anti CD86 antibody (Cat#: GTX32507; 1:100; GeneTex., CA, USA) or anti CD163 antibody (Cat#: GTX35247; 1:100; GeneTex., CA, USA) at 4 °C overnight. Subsequently, the sections were rinsed with PBS, then incubation of the secondary antibody HRP Envision kit (DAKO, CA, USA) for 20 min. Afterwards, sections were rinsed again and incubated for 15 min with

3,3'-diaminobenzidine tetrahydrochloride (DAB Substrate Kit, CA, USA). Finally, sections were counterstained with hematoxylin, dehydrated and cleared in xylene then cover-slipped for microscopic analysis. Six non-overlapping random fields from CA3 region were scanned and investigated to assess CD86 and CD163 mean positive count of reactive microglial cells in immuno-stained tissue sections [42], using Leica Application system modules for histological analysis (Leica Microsystems GmbH, Wetzlar, Germany).

### 2.9. Statistical analysis

Statistical analysis was implemented via the statistical software package GraphPad Prism®, Version 9.00 for Windows (California, USA), using one-way ANOVA test followed by Tukey's post hoc test. The data were demonstrated as mean ± standard deviation (SD). For all tests, the level of significance was set at p-value < 0.05.

## 3. Results

### 3.1. CANA attenuated MTX-induced cognitive deficits

MTX induced behavioral and memory impairment that was witnessed in NOR and MWM tests [Fig. 2 & 3]. Indeed, MTX reduced DI by 1.6-fold and PI by 66 % in NOR test, as compared to control group. In parallel, MTX increased latency time to reach target quadrant by 1.8-folds along with reduction in time spent in target quadrant and path efficiency by 50 and 57 % in MWM test, relative to control group. On the other hand, treatment with CANA mitigated behavioral and cognitive deficits and enhanced both DI and PI in NOR by 2.2- and 1.5-folds, respectively relative to the MTX-group. In addition, CANA reduced latency time by 43 % and increased both; time spent in target quadrant (1.65-folds) and path efficiency (2.15-folds) in MWM, as compared to the insult group.

### 3.2. CANA improved MTX-induced histopathological impairments

Hematoxylin and eosin stain of hippocampal control rats demonstrated well organized morphological features of CA3 layers with apparent intact pyramidal neurons and intercellular brain matrix with minimal glial cells infiltrates. In opposition, MTX samples revealed

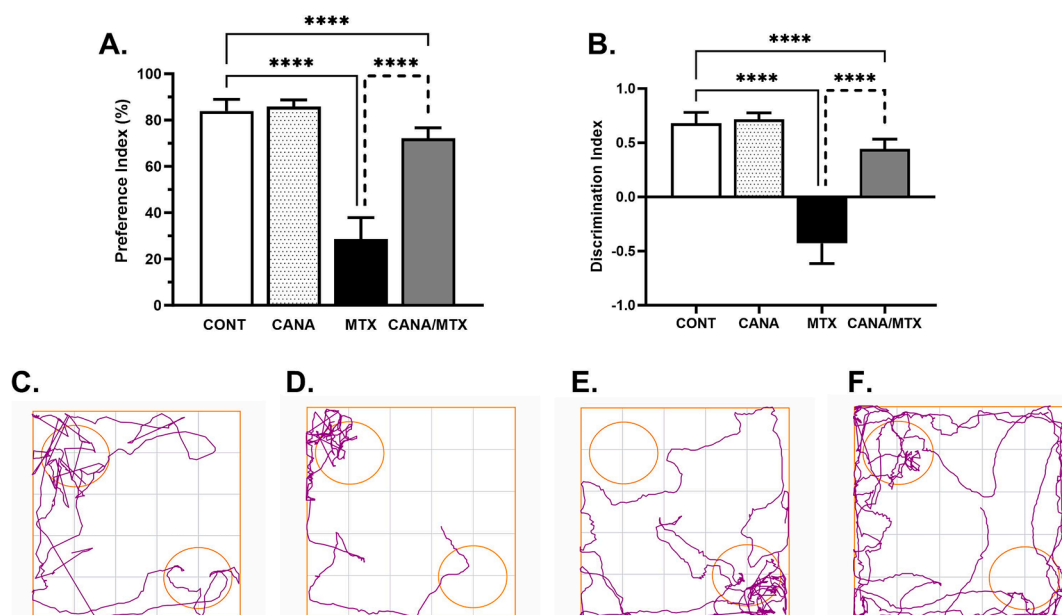


**Fig. 2.** Effect of CANA on MTX-induced cognitive impairment observed in NOR test. Panels represent discrimination index (A), preference index (B) and descriptive track plots during NOR test (C). Data are expressed as mean ± SD (n = 12/group), using one-way ANOVA followed by Tukey's post hoc test; \*\*\*\* p < 0.0001.



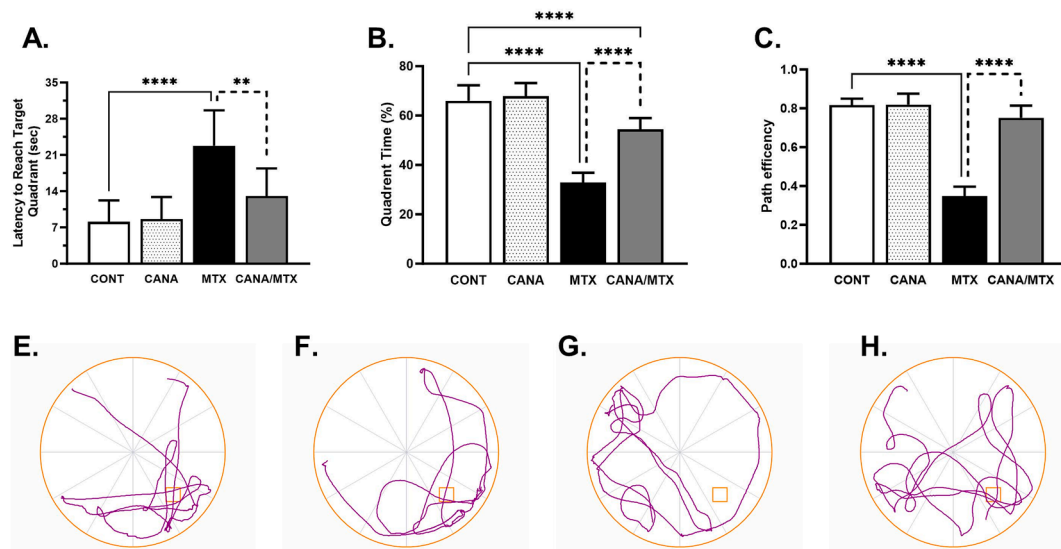


**Fig. 3.** Effect of CANA on MTX-induced cognitive impairment observed in MWM test. Panels represent latency time (A), time spent in target quadrant (B), path efficiency (C) and descriptive track plots during NOR test (D). Data are expressed as mean  $\pm$  SD (n = 12/group), using one-way ANOVA followed by Tukey's post hoc test; \*\* p < 0.01, \*\*\*\* p < 0.0001. CANA: canagliflozin; MTX: methotrexate; MWM: Morris water maze.

severe diffuse neuronal loss and degenerative changes records with abundant records of shrunken hyperesophilic pyknotic neurons losing their subcellular details. In addition, moderate perineuronal edema as well as edema of brain matrix were observed with moderate higher records of reactive microglial cells infiltrates. Treatment with CANA demonstrated a neuroprotective efficacy with a significant higher record of apparent intact neurons with organized histological features and minimal sporadic records of degenerated neurons reactive glial cells infiltrates were observed [Fig. 4].

### 3.3. CANA ameliorated MTX-induced redox status abnormalities

As depicted in Fig. 5, MTX administration evoked an oxidative stress status that was witnessed by marked upsurge in lipid peroxidation marker, MDA, by 2.2-folds along with obvious reduction in antioxidant defense mechanism as verified by a reduction in reduced GSH content by 50 %, as well as SOD and GPx activities by 49 and 59 %, respectively as compared to control group. In opposition, CANA proved its antioxidant capability and lowered MDA content by 57 % together with marked increment in reduced GSH content and SOD and GPx activities by 55, 65 and 112 %, respectively relative to the insult.

### 3.4. CANA mitigated MTX-induced NLRP3 inflammasome activation and apoptotic biomarker

The oxidative stress status associated with MTX administration triggered the release of DAMP such as HMGB1 and upregulation of TLR-4. Activation of the latter recruits adaptor proteins that eventually leads to activation of NF $\kappa$ B p65 and provoking a neuroinflammatory status [Fig. 6]. Indeed, MTX increased HMGB1 protein content by 4.3-folds along with increment in the protein expression of TLR4 and p-NF $\kappa$ B p65 by 4.0 and 4.2-folds, respectively as compared to control group. Consequently, NLRP3 signal transduction proteins were extremely expressed, as witnessed by 6.0 and 2.3-folds increase in the protein expression of NLRP3 and ASC. In parallel, MTX boosted the apoptotic flux as evidenced by increasing the protein expression of caspase-1 by 3.5-folds and the protein content of IL-1 $\beta$  and IL-8 by 1.6- and 2.1-folds, as compared to control group [Fig. 7]. On the other hand, CANA reduced the neuroinflammation induced by MTX mainly via NLRP3 inflammasome. In CANA-treated group, HMGB1, TLR4, p-NF $\kappa$ B p65, NLRP3 and ASC protein expressions were decreased by 54, 60, 56, 55 and 58 %, respectively as compared to MTX-group. Moreover, CANA suppressed apoptosis as demonstrated by obvious reduction in caspase-1

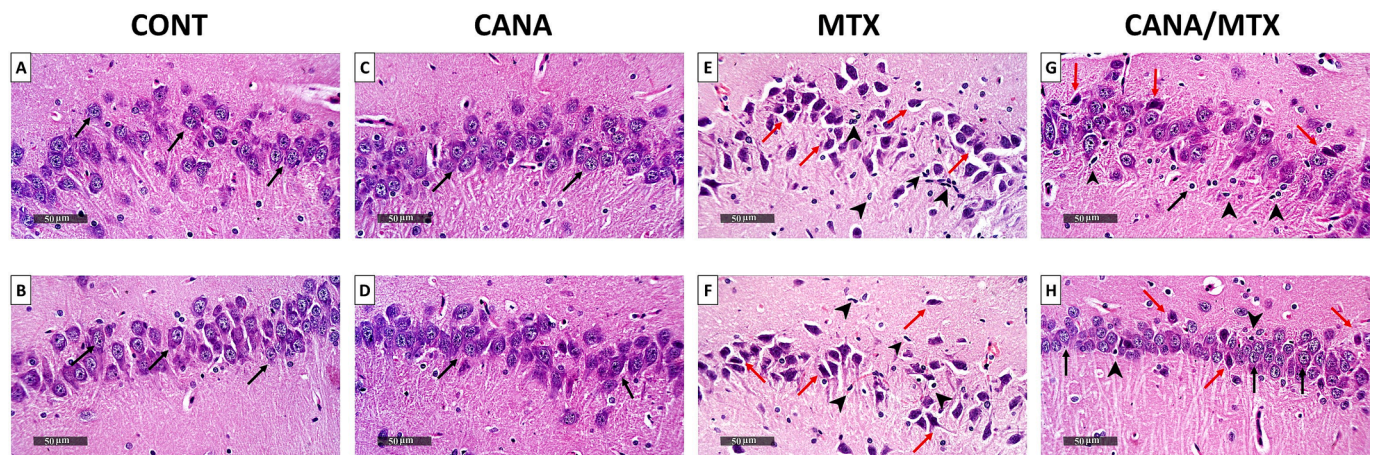


**Fig. 4.** Effect of CANA on MTX-induced histopathological impairments. Photomicrographs represent H&E staining of CA3 area of hippocampus from (a) control group, (b) CANA control rats, (c) MTX group and (d) CANA-treated group. CANA: canagliflozin; MTX: methotrexate.

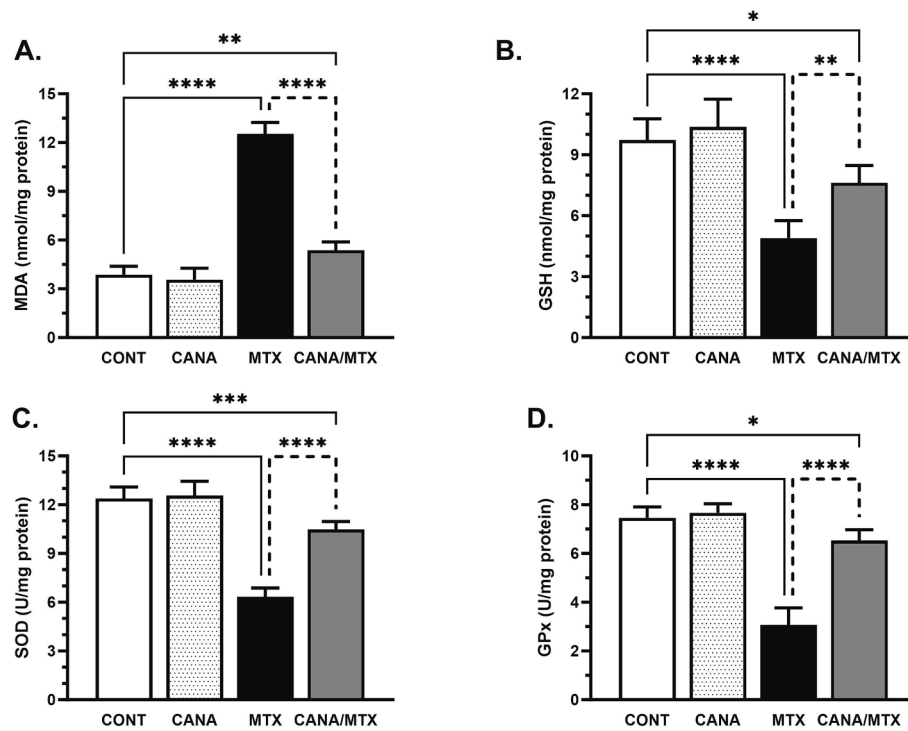


**Fig. 5.** Effect of CANA on hippocampal MDA (A), reduced GSH (B), SOD (C) and GPx (D) in MTX-induced cognitive impairment. Data are expressed as mean  $\pm$  SD ( $n = 6$ /group); statistical analysis was performed using one-way ANOVA followed by Tukey's post hoc test; \*  $p < 0.05$ , \*\*  $p < 0.01$ , \*\*\*  $p < 0.001$ , \*\*\*\*  $p < 0.0001$ . CANA: canagliflozin; MTX: methotrexate; MDA: malondialdehyde; GSH: glutathione; SOD: superoxide dismutase; GPx: glutathione peroxidase.

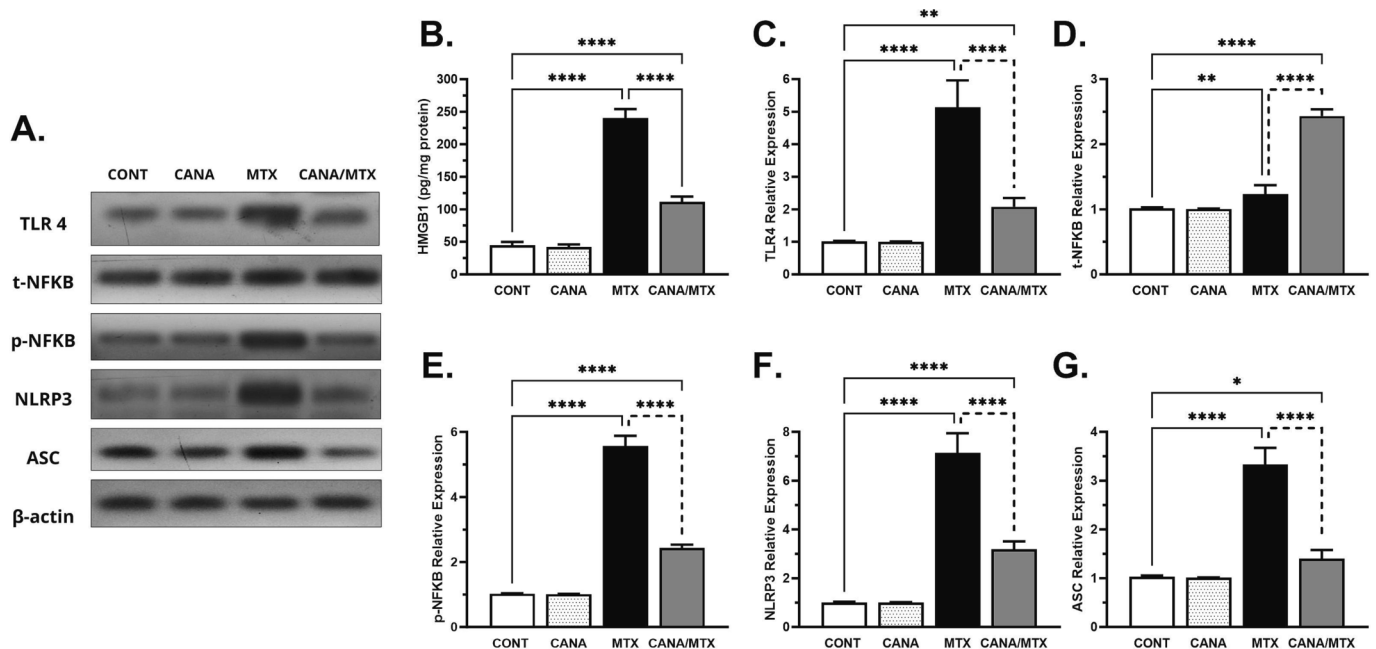


**Fig. 6.** Effect of CANA on hippocampal HMGB1 content (B), as well as the protein expression of TLR4 (C), t-NFκB (D), p-NFκB (E), NLRP3 (F) and ASC (G) in MTX-induced cognitive impairment. Panel (A) represents western blots bands for the protein expressions. Data are expressed as mean  $\pm$  SD ( $n = 3-6$ /group); statistical analysis was performed using one-way ANOVA followed by Tukey's post hoc test; \*  $p < 0.05$ , \*\*  $p < 0.01$ , \*\*\*  $p < 0.001$ , \*\*\*\*  $p < 0.0001$ . CANA: canagliflozin; MTX: methotrexate; HMGB1: high mobility group box-1; TLR4: toll like receptor-4; NFκB: nuclear factor kappa B.

protein expression together with IL-1 $\beta$  and IL-8 protein contents by 60, 46 and 47 %, respectively relative to the insult.

### 3.5. CANA modulated MTX-induced macrophage polarization dysregulation (M1/M2)

In Figs. 8–10, administration of MTX was coupled with neuro-inflammation via shifting M1/M2 macrophage polarization to M1 cascade as witnessed by an increase in iNOS content by 12.5-folds and

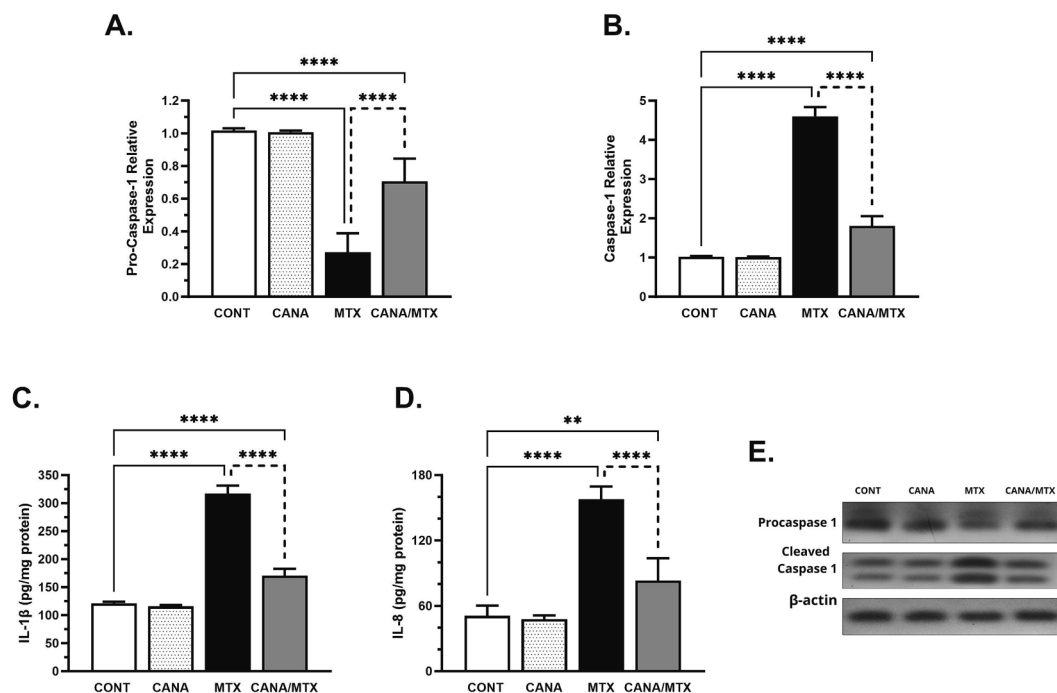


**Fig. 7.** Effect of CANA on hippocampal protein expression of procaspase-1 (A), caspase-1 (B), as well as protein content of IL-1 $\beta$  (C) and IL-8 (D) in MTX-induced cognitive impairment. Data are expressed as mean  $\pm$  SD ( $n = 3-6$ /group); statistical analysis was performed using one-way ANOVA followed by Tukey's post hoc test; \*\*  $p < 0.01$ , \*\*\*\*  $p < 0.0001$ . CANA: canagliflozin; MTX: methotrexate; IL-1 $\beta$ : interleukin-1 $\beta$ ; IL-8: interleukin-8.

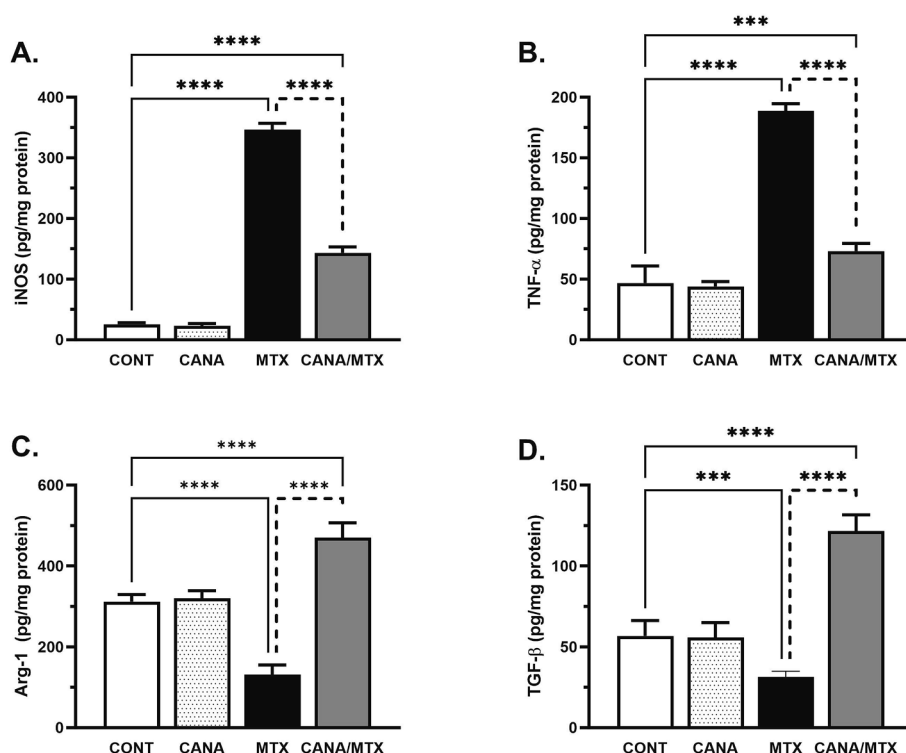


**Fig. 8.** Effect of CANA on hippocampal protein contents of iNOS (A), TNF- $\alpha$  (B), arginase (C) and TGF- $\beta$  (D) in MTX-induced cognitive impairment. Data are expressed as mean  $\pm$  SD ( $n = 6$ /group); statistical analysis was performed using one-way ANOVA followed by Tukey's post hoc test; \*\*\*  $p < 0.001$ , \*\*\*\*  $p < 0.0001$ . CANA: canagliflozin; MTX: methotrexate; iNOS: inducible nitric oxide synthase; TNF- $\alpha$ : tumor necrosis factor-alpha; TGF $\beta$ : transforming growth factor $\beta$ .

TNF- $\alpha$  contents by 3-folds as well as hippocampal CD86 immunoreactivity by 7.2-folds. In parallel, arginase-1 (Arg-1) and TGF- $\beta$  protein contents were reduced by 60 and 50 %, respectively along with hippocampal CD163 immunoreactivity by 75 %. In contrast, CANA

demonstrated an anti-inflammatory capability via directing M1/M2 macrophage polarization towards M2 phenotype as demonstrated by a reduction in iNOS content by 59 % and TNF- $\alpha$  contents by 61 %, respectively together with CD86 immunoreactivity by 70 %. In addition,

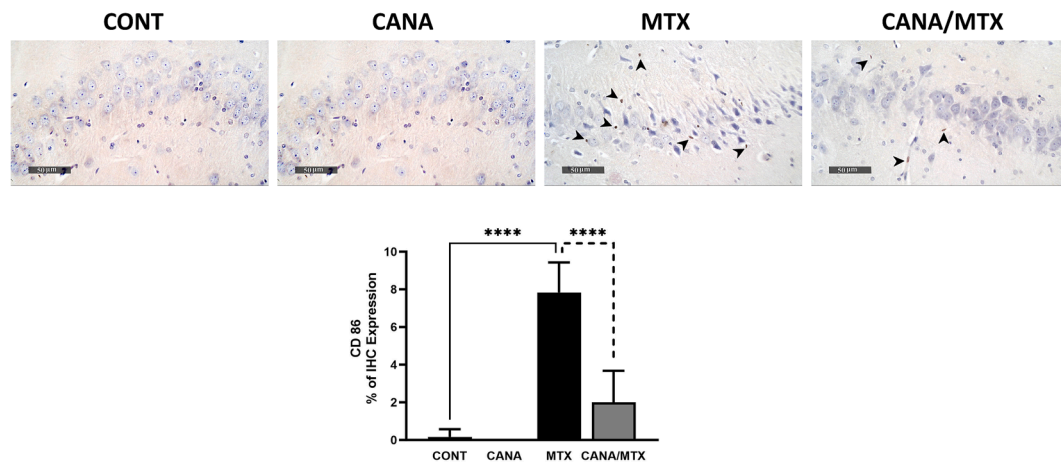


**Fig. 9.** Effect of CANA on hippocampal CD86 immunoreactivity in MTX-induced cognitive impairment. Photomicrographs represent control group (A), CANA control rats (B), MTX group (C) and (D) CANA-treated group (D). Panel (E) demonstrated % of immunohistochemical expression of CD86. Data are expressed as mean  $\pm$  SD ( $n = 3/\text{group}$ ); statistical analysis was performed using one-way ANOVA followed by Tukey's post hoc test; \*\*\*\*  $p < 0.0001$ . CANA: canagliflozin; MTX: methotrexate.

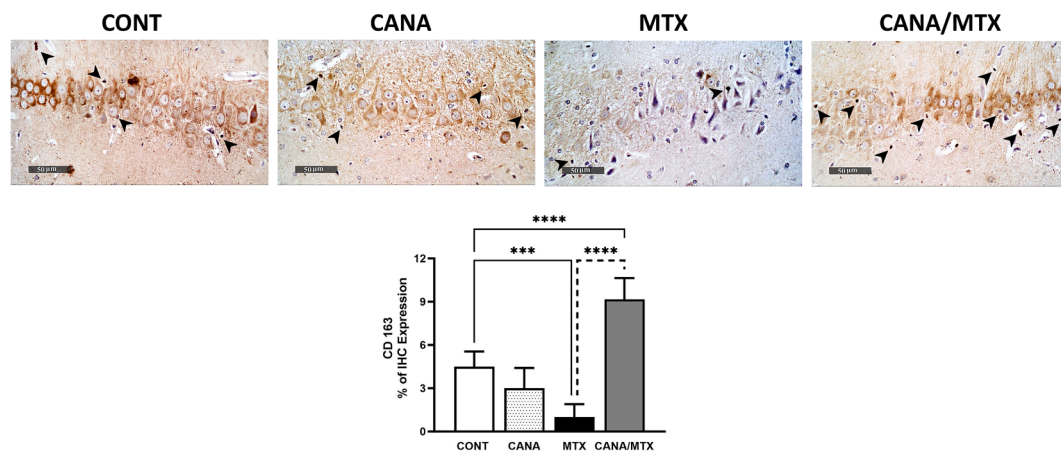


**Fig. 10.** Effect of CANA on hippocampal CD163 immunoreactivity in MTX-induced cognitive impairment. Photomicrographs represent control group (A), CANA control rats (B), MTX group (C) and (D) CANA-treated group (D). Panel (E) demonstrated % of immunohistochemical expression of CD163. Data are expressed as mean  $\pm$  SD ( $n = 3/\text{group}$ ); statistical analysis was performed using one-way ANOVA followed by Tukey's post hoc test; \*\*\*  $p < 0.001$ , \*\*\*\*  $p < 0.0001$ . CANA: canagliflozin; MTX: methotrexate.

an increase in Arg-1 content by 2.7-folds and TGF- $\beta$  contents by 2.9-folds as well as CD163 immunoexpression by 8-folds were observed in comparison with MTX-group.

### 3.6. CANA attenuates neuroinflammation via regulating TLR4/NF- $\kappa$ B/NLRP3 transcription Factors: Extensive bioinformatic approach

Using the Pathway Studio® bioinformatic freely available tool (<https://www.pathwaystudio.com>), we investigated the possible interactions between MTX, CANA, and apoptosis. TLR4, MyD88, NF- $\kappa$ B, NLRP3 and inflammasome were included in our research since they are known to be involved in the control of the inflammasome and inflammation process. Complex interactions between the previously listed medications, receptors, regulators, and transcription factors have been identified as shown in Fig. 11. Our bioinformatics studies showed that MTX directly stimulates the expression of TLR4, NF- $\kappa$ B, and NLRP3. In addition to having a direct positive regulatory impact apoptosis, MTX upregulate inflammasome which also activates apoptosis. It is important to point out that the observed MTX downregulatory effect on TLR4 is based on adipose tissue studies [43]. CANA, on the other hand, turned out to be a direct inhibitor of NF- $\kappa$ B expression as well as a down regulator of

NLRP3 and the inflammasome. Noteworthy, the regulatory effect of CANA on the apoptosis process is still unknown and is based on diverse studies made on different tissues and cell types other than ours [30,44]. In general, our bioinformatics data indicates that TLR4 actively binds and stimulates MyD88 and NF- $\kappa$ B, which directly upregulate the expression of both NLRP3 and the inflammasome and induce the binding of NLRP3 to the inflammasome, triggering inflammation and apoptosis.

## 4. Discussion

This study represents the first investigation into the molecular impact of MTX, both as a standalone treatment and in combination with CANA. Furthermore, this study offers compelling in vivo evidence demonstrating the efficacy of CANA in mitigating the neurotoxic effects triggered by MTX specifically in the rats. CANA, a SGLT2 inhibitor, has demonstrated intriguing anti-inflammatory characteristics in various models of lungs and liver toxicity as well as pneumonia diabetic patients [28–30]. A recent study performed at our laboratory has demonstrated the potential benefits of CANA as a neuroprotective drug for the treatment and prevention of neurodegenerative diseases. The observed effect



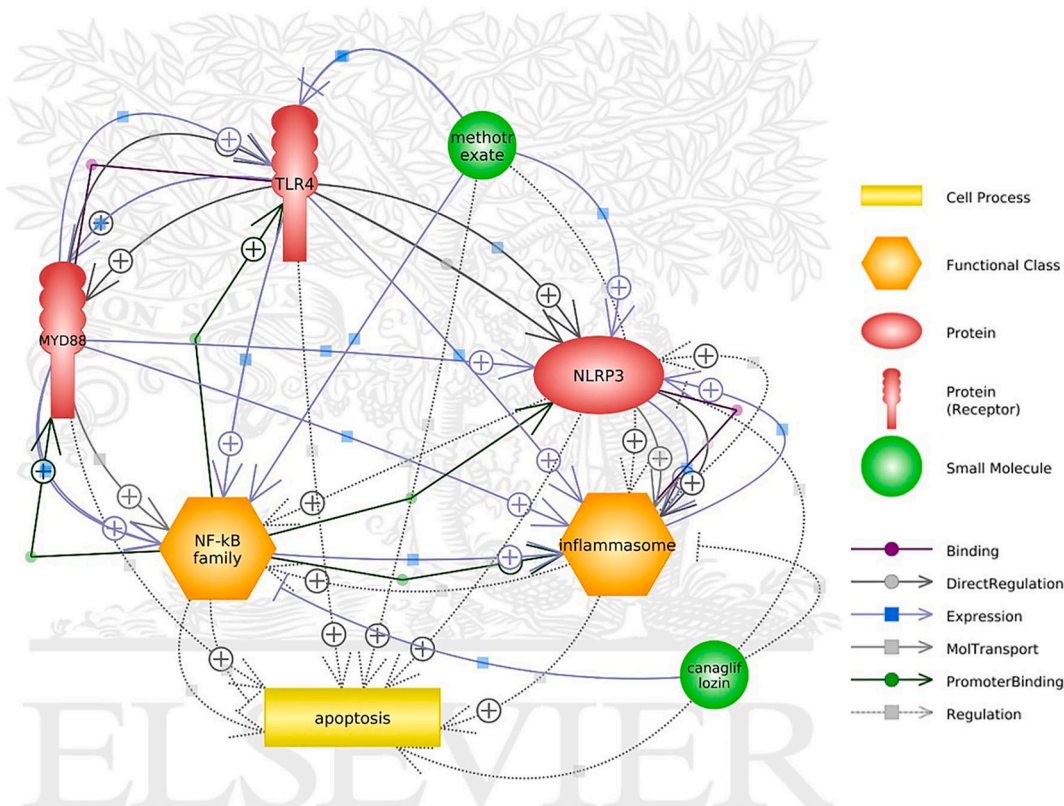


**Fig. 11.** Network analysis of MTX, Canagliflozin, TLR4, MyD88, NF- $\kappa$ B, NLRP3, inflammasome and apoptosis Process. The generated network demonstrated that TLR4 actively binds and promotes MyD88 and NF- $\kappa$ B, which directly upregulate both NLRP3 and the inflammasome and induce the binding of NLRP3 to the inflammasome, triggering inflammation and apoptosis.

was attributed to the upregulatory activity of CANA on autophagic pathways [45]. Likewise, the current work offers further proof of the neuroprotective properties of CANA in mitigating the neurotoxic effects induced by MTX. A bioinformatic analysis was conducted to explore the potential pathway for our *in vivo* study. The bioinformatic analysis conducted in our study has identified a potential direct stimulatory action of MTX on TLR4, NF- $\kappa$ B, and NLRP3, leading to the activation of apoptosis. In contrast, the findings indicate that CANA may have a direct inhibitory effect on NLRP3 and inflammasome, hence potentially contributing to its protective, anti-inflammatory effects. These effects may be attributed to the modulation of the hippocampal TLR4/MyD88/NF- $\kappa$ B/NLRP3 inflammasome signaling pathway.

At the end of the specified experimental time, the behavioral analysis was carried out, which included conducting both the NOR and MWM tests. Both trials consistently demonstrated a statistically significant decrease in cognitive function and memory in rats who were administered MTX therapy. Nevertheless, a notable enhancement in these capabilities was noted when the administration of CANA coincided with MTX. The NOR test revealed that the MTX group exhibited a notable decrease in both the DI and PI, which is consistent with findings reported in earlier studies investigating the neurotoxic effects of MTX [36]. In the context of the MWM experiment, it was shown that the administration of MTX resulted in a comparable decline in cognitive performance. This was demonstrated by the notable rise in latency time and decrease in quadrant time and path efficiency. The outcomes of the MTX group in both NOR and MWM exhibited similarities to the findings reported in more recent studies [6,7]. On the contrary, the co-treatment with CANA demonstrated a notable enhancement in cognitive performance. Both the DI and PI exhibited a significant rise of 2.2-fold and 15-fold, respectively, in comparison to the MTX group. Moreover, there was a notable decrease in latency time, accompanied by a substantial gain in quadrant time and path efficiency, with respective fold changes of 1.65

and 2.15 when compared to MTX group.

Subsequently, histological and immunohistochemical analyses were conducted. The histopathological examination using H&E staining revealed a notable reduction in neuronal density and an elevated level of neurodegeneration in the group treated with MTX, as compared to the control group. Additionally, we noticed a slight increase in the count of activated microglia. The findings presented in this study corroborate prior research that reported a notable reduction in the number of neurons in the dentate gyrus (DG) and CA3 regions of the hippocampus, as well as an elevation in microglial activation [6,7]. In contrast, the group that received co-treatment with CANA exhibited a notable preservation of neuronal count and little evidence of reactive glial cell infiltration. The immunohistochemistry analysis demonstrated a transition occurring between the M1 and M2 phenotypes of microglia. The M1 phenotype is characterized by its pro-inflammatory features, whereas the M2 phenotype is related with anti-inflammatory properties and has been shown to confer neuroprotective effects [25,46]. CD86 marker was identified as a marker of identifying the M1 neuroinflammatory phenotypic polarization while the polarization of M2 phenotype was identified with the use of CD163 [47–49]. In MTX group we detected an increase in M1 polarization in comparison to M2 polarization. This is evidenced by the increase in CD86 and decrease of CD163 expression. This M1/M2 polarization is in line with previously mentioned data correlating the increase in M1 activation with the pathophysiology of Alzheimer's disease [50]. In CANA co-treated group M2 polarization was significantly increased thus increasing CD163 expression over CD86 marker of M1 which supports the importance of maintaining M1/M2 polarization as an approach to prevent and treat neurodegenerative diseases [51].

To validate the findings, the protein level of iNOS was measured as an indicator for M1 polarization, whereas Arg-1 was measured as an indicator for M2 polarization using the ELISA approach. A notable

elevation in iNOS expression was seen, alongside a reduction in Arg-1 protein levels, within the MTX group as compared to the normal control. The upregulation of M1 microglia activation and downregulation of M2 microglia were associated with an elevation in the TNF- $\alpha$  and a decrease in the TGF- $\beta$ . These findings align with previous research indicating that M1 microglia increase in relation to MTX-treated inflammatory diseases such as rheumatoid arthritis and pulmonary injury, leading to elevated levels of TNF- $\alpha$  [52,53], whereas the protein content analysis conducted on samples co-treated with CANA revealed a notable increase in the levels of TGF- $\beta$  and Arg-1, alongside TNF- $\alpha$  and iNOS reduction. This effect of CANA came in alignment with the published data proving its antioxidant cardioprotective effect [54]. TGF- $\beta$  serves as both an anti-inflammatory mediator and a promoter of M2 microglia autoactivation, hence enhancing its neuroprotective capabilities [48,55]. Furthermore, TGF- $\beta$  and Arg-1 were found to elevate as a neuroprotective effect of hesperidin treated ischemic stroke model [56].

The production of inflammatory cytokines by M1 microglia stimulated by MTX appears to be accompanied with an elevation in oxidative stress. This was demonstrated by a marked rise in MDA expression, over twice the level detected in the normal control group. Additionally, there was a notable decrease in the activity of GSH, SOD, and GPx, reaching around 50–60 % of their normal control activity levels. These results of this study align with prior research that has emphasized the oxidative power of MTX [57,58]. The administration of MTX led to the creation of oxidative stress, resulting in the release of HMGB1 and the upregulation of TLR4, which exhibited a four-fold increase in expression compared to their baseline levels. Consequently, this activation of TLR4 prompted the activation of NF- $\kappa$ B p65. Similarly, it was proved that MTX has the ability to stimulate the activation of NF- $\kappa$ B p65 through the upregulation of the TLR4/MYD88 pathway in a model of MTC-induced cardiotoxicity [59]. The activation of NF- $\kappa$ B is understood to be facilitated by MYD88, leading to the cytosolic phosphorylation of inhibitor molecules bound to NF- $\kappa$ B and subsequently liberates NF- $\kappa$ B for nuclear translocation thus, initiating the transcription for genes involved in inflammatory processes [60]. Among these genes are the NLRP3 and ASC which are essential for the formation of the NLRP3 inflammasome.

The increased NLRP3 inflammasome increases the cleavage of pro-caspase-1 into activated caspase-1 which in return activates pro-IL-1 $\beta$  and pro-IL-18 into IL-1 $\beta$  and IL-18. This was evidenced by the significant increase in the expression of caspase-1, IL-1 $\beta$  and IL-18 by 3.5, 1.6 and 2.1 folds respectively. Caspase-1 and its downstream IL-1 $\beta$  and IL-18 are well known to induce apoptosis, pyroptosis and inflammation [61]. Furthermore, the increased NLRP3 inflammasome plays a crucial role in altering the M1/M2 balance, increasing the inflammatory M1 microglia [62]. Thus, closing a loop of inflammatory response induced by MTX. On the contrary, CANA proved itself to be a promising co-treatment that can break this inflammatory loop.

CANA exhibited a neuroprotective and anti-inflammatory effect by effectively decreasing the production of HMGB1 and the expression of TLR4. This reduction led to a significant decrease in the downstream MYD88 activity, resulting in a 56 % reduction in the activation and translocation of NF- $\kappa$ B p65 compared to the normal control. This would lead to the suppression of NLRP3 and ASC gene expression, as well as the formation of NLRP3 inflammasome. The decrease in NLRP3 inflammasome assembly leads to a reduction in the activation of pro-caspase-1, pro-IL-1 $\beta$ , and pro-IL-18. The protective effect of this process has been demonstrated in studies, showing its ability to provide protection against cardiovascular and neurological damage, as well as its anti-inflammatory properties in cases of stress and lipopolysaccharide-induced inflammation [33,63–65]. Additionally, a decrease in the production of NLRP3 inflammasome leads to a beneficial transition from M1 to M2 microglial activation [66]. The polarization of M2 macrophages leads to an anti-inflammatory and antioxidant impact. It was clearly demonstrated by the 57 % reduction in lipid peroxidation (i.e. MDA) as compared to MTX monotherapy. likewise, the observed elevation in GSH, SOD, and GPx levels is consistent with the documented

antioxidant properties of CANA [54,67].

In conclusion, our study explored the inflammatory, apoptotic, and pyroptotic effects of MTX. The neurotoxic effects of MTX were observed across various levels of study, including behavioral, histological, and biochemical analyses. The observed effect can be ascribed to the activation of the TLR4/MyD88/NF- $\kappa$ B/NLRP3 pathway, resulting in the stimulation of M1 microglial cells and the induction of oxidative stress. The presence of oxidative stress causes the production of HMGB1, which then enhances the expression of TLR4, resulting in a self-perpetuating cycle of inflammatory response and apoptosis. The efficacy of CANA in disrupting this cycle has been revealed by its ability to attenuate the TLR4/MyD88/NF- $\kappa$ B/NLRP3 pathway, resulting in a decrease in the production of the NLRP3 inflammasome and its downstream apoptotic elements, including caspase-1, IL-1 $\beta$ , and IL-18. Additionally, this effect resulted in an adjustment of microglial polarization from the M1 phenotype to the M2 phenotype, hence suppressing the occurrence of apoptosis, pyroptosis, and inflammatory responses induced by MTX. Thus, it has been proved that CANA has the potential to serve as an effective co-treatment option alongside MTX in order to mitigate its neurotoxic effects.

## Funding

This research did not receive any specific grant from funding agencies in the public, commercial, or not for profit sector.

## CRediT authorship contribution statement

**Lobna H. Khedr:** Writing – review & editing, Supervision, Methodology, Formal analysis, Data curation, Conceptualization. **Rania M. Rahmo:** Writing – review & editing, Supervision, Investigation, Conceptualization. **Omar M. Eldemerdash:** Writing – original draft, Formal analysis, Data curation, performing Bioinformatic analysis in authorship contribution. **Engy M. Helmy:** Investigation, Data curation. **Felopateer A. Ramzy:** Investigation, Data curation. **George H. Lotfy:** Investigation, Data curation. **Habiba A. Zakaria:** Investigation, Data curation. **Marine M. Gad:** Investigation, Data curation. **Marina M. Youhanna:** Investigation, Data curation. **Manar H. Samaan:** Investigation, Data curation. **Nevert W. Thabet:** Investigation, Data curation. **Reem H. Ghazal:** Investigation, Data curation. **Mostafa A. Rabie:** Writing – review & editing, Supervision, Investigation, Formal analysis, Data curation.

## Declaration of competing interest

The authors declare that they have no known competing financial interests or personal relationships that could have appeared to influence the work reported in this paper.

## Data availability

Data will be made available on request.

## References

- [1] M. Visentin, R. Zhao, I.D. Goldman, The antifolates, *Hematol. Oncol. Clin. N. Am.* 26 (3) (2012) 629, <https://doi.org/10.1016/j.hoc.2012.02.002>.
- [2] J.B. Stone, L.M. DeAngelis, Cancer-treatment-induced neurotoxicity—focus on newer treatments, *Nat. Rev. Clin. Oncol.* 13 (2) (2016) 92.
- [3] J. John, M. Kinra, J. Mudgal, G. Viswanatha, K. Nandakumar, Animal models of chemotherapy-induced cognitive decline in preclinical drug development, *Psychopharmacology* 238 (11) (2021) 3025.
- [4] J. Dietrich, M. Prust, J. Kaiser, Chemotherapy, cognitive impairment and hippocampal toxicity, *Neuroscience* 309 (2015) 224, <https://doi.org/10.1016/j.neuroscience.2015.06.016>.
- [5] J.U. Welbat, S. Naewla, W. Pannangrong, A. Sirichoat, A. Aranarochana, P. Wigmore, Neuroprotective effects of hesperidin against methotrexate-induced changes in neurogenesis and oxidative stress in the adult rat, *Biochem. Pharmacol.* 178 (2020) 114083, <https://doi.org/10.1016/j.bcp.2020.114083>.

- [6] M. Taha, O.M. Eldemerdash, I.M. Elshaffei, E.M. Yousef, M.A. Senousy, Dexmedetomidine Attenuates Methotrexate-Induced Neurotoxicity and Memory Deficits in Rats through Improving Hippocampal Neurogenesis: The Role of miR-15a/ROCK-1/ERK1/2/CREB/BDNF Pathway Modulation, *Int. J. Mol. Sci.* 24 (1) (2023) 766, <https://doi.org/10.3390/ijms24010766>.
- [7] M. Taha, O.M. Eldemerdash, I.M. Elshaffei, E.M. Yousef, A.S. Soliman, M. A. Senousy, Apigenin Attenuates Hippocampal Microglial Activation and Restores Cognitive Function in Methotrexate-Treated Rats: Targeting the miR-15a/ROCK-1/ERK1/2 Pathway, *Mol. Neurobiol.* 60 (7) (2023) 3770–3787, <https://doi.org/10.1007/s12035-023-03299-7>.
- [8] H. Wu, R. Li, Z.-H. Wei, X.-L. Zhang, J.-Z. Chen, Q. Dai, J. Xie, B. Xu, Diabetes-induced oxidative stress in endothelial progenitor cells may be sustained by a positive feedback loop involving high mobility group box-1, *J. Oxidative Med. Cellular Longevity* (2016).
- [9] M. He, M.E. Bianchi, T.R. Coleman, K.J. Tracey, Y. Al-Abed, Exploring the biological functional mechanism of the HMGB1/TLR4/MD-2 complex by surface plasmon resonance, *J. Mol. Med.* 24 (1) (2018) 1–9.
- [10] A.M. Schmidt, S. Du Yan, S.F. Yan, D.M. Stern, The biology of the receptor for advanced glycation end products and its ligands, *Biochim. Et Biophys. Acta –Mol. Cell Res.* 1498 (2–3) (2000) 99–111.
- [11] H. Ahmed, M.A. Khan, U.D. Kahlert, M. Niemelä, D. Hänggi, S.R. Chaudhry, A. Muhammad, Role of Adaptor Protein Myeloid Differentiation 88 (MyD88) in Post-Subarachnoid Hemorrhage Inflammation: A Systematic Review, *Int. J. Mol. Sci.* 22 (8) (2021), <https://doi.org/10.3390/ijms22084185>.
- [12] Q. Wang, Q. Luo, Y.H. Zhao, X. Chen, Toll-like receptor-4 pathway as a possible molecular mechanism for brain injuries after subarachnoid hemorrhage, *Int. J. Neurosci.* 130 (9) (2020) 953–964, <https://doi.org/10.1080/00207454.2019.1709845>.
- [13] Y. Yang, H. Wang, M. Kouadir, H. Song, F. Shi, Recent advances in the mechanisms of NLRP3 inflammasome activation and its inhibitors, *Cell Death Dis.* 10 (2) (2019) 128, <https://doi.org/10.1038/s41419-019-1413-8>.
- [14] J.C. Leemans, L. Kors, H.-J. Anders, S. Florquin, Pattern recognition receptors and the inflammasome in kidney disease, *Nat. Rev. Nephrol.* 10 (7) (2014) 398–414.
- [15] A. Loverre, P. Dittonno, A. Crovace, L. Gesualdo, E. Ranieri, P. Pontrelli, G. Stallone, B. Infante, A. Schena, S. Di Paolo, Ischemia-reperfusion induces glomerular and tubular activation of proinflammatory and antiapoptotic pathways: differential modulation by rapamycin, *J. Am. Soc. Nephrol.* 15 (10) (2004) 2675–2686.
- [16] S.M. Abd El-Twab, O.E. Hussein, W.G. Hozayen, M. Bin-Jumah, A.M. Mahmoud, Cholic acid prevents methotrexate-induced kidney injury by suppressing NF-κB/NLRP3 inflammasome activation and up-regulating Nrf2/ARE/HO-1 signaling, *Inflamm. Res.* 68 (6) (2019) 511–523, <https://doi.org/10.1007/s00011-019-01241-z>.
- [17] Q. He, H. You, X.-M. Li, T.-H. Liu, P. Wang, B.-E. Wang, HMGB1 promotes the synthesis of pro-IL-1β and pro-IL-18 by activation of p38 MAPK and NF-κB through receptors for advanced glycation end-products in macrophages, *Asian Pac. J. Cancer Prev.* 13 (4) (2012) 1365–1370.
- [18] J. Tschopp, K. Schroder, NLRP3 inflammasome activation: The convergence of multiple signalling pathways on ROS production? *Nat. Rev. Immunol.* 10 (3) (2010) 210–215, <https://doi.org/10.1038/nri2725>.
- [19] Z. Chen, Z. Wang, Y. Hu, H. Lin, L. Yin, J. Kong, Y. Zhang, B. Hu, T. Li, X. Zheng, Q. Yang, S. Ye, S. Wang, Q. Zhou, C. Zheng, ELABELA/APJ Axis Prevents Diabetic Glomerular Endothelial Injury by Regulating AMPK/NLRP3 Pathway, *Inflammation* (2023), <https://doi.org/10.1007/s10753-023-01882-7>.
- [20] J. Barrington, E. Lemarchand, S.M. Allan, A brain in flame: do inflammasomes and pyroptosis influence stroke pathology? *Brain Pathol.* 27 (2) (2017) 205–212.
- [21] S.W. Lee, J.P. de Rivero Vaccari, J.S. Truettner, W.D. Dietrich, R.W. Keane, The role of microglial inflammasome activation in pyroptotic cell death following penetrating traumatic brain injury, *J. Neuroinflammation* 16 (1) (2019) 1–12.
- [22] X. Ming, W. Li, Y. Maeda, B. Blumberg, S. Raval, S.D. Cook, P.C. Dowling, Caspase-1 expression in multiple sclerosis plaques and cultured glial cells, *J. Neurol. Sci.* 197 (1–2) (2002) 9–18, [https://doi.org/10.1016/s0022-510x\(02\)00030-8](https://doi.org/10.1016/s0022-510x(02)00030-8).
- [23] S. Moonen, M.J. Koper, E. Van Schoor, J.M. Schaeferbeke, R. Vandenbergh, C.A. F. van Armin, T. Tousseyn, B. De Strooper, D.R. Thal, Pyroptosis in Alzheimer's disease: cell type-specific activation in microglia, astrocytes and neurons, *Acta Neuropathol.* 145 (2) (2023) 175–195, <https://doi.org/10.1007/s00401-022-02528-y>.
- [24] M. Cowan, W.A. Petri Jr., Microglia: Immune Regulators of Neurodevelopment, *Front. Immunol.* 9 (2018) 2576, <https://doi.org/10.3389/fimmu.2018.02576>.
- [25] R. Shechter, O. Miller, G. Yovel, N. Rosenzweig, A. London, J. Ruckh, K.-W. Kim, E. Klein, V. Kalchenko, P. Bendel, Recruitment of beneficial M2 macrophages to injured spinal cord is orchestrated by remote brain choroid plexus, *Immunity* 38 (3) (2013) 555–569.
- [26] C.T. Jiang, W.F. Wu, Y.H. Deng, J.W. Ge, Modulators of microglia activation and polarization in ischemic stroke (Review), *Mol. Med. Rep.* 21 (5) (2020) 2006–2018, <https://doi.org/10.3892/mmr.2020.11003>.
- [27] H.J.L. Heerspink, P. Perco, S. Mulder, J. Leierer, M.K. Hansen, A. Heinzel, G. Mayer, Canagliflozin reduces inflammation and fibrosis biomarkers: a potential mechanism of action for beneficial effects of SGLT2 inhibitors in diabetic kidney disease, *Diabetologia* 62 (7) (2019) 1154–1166, <https://doi.org/10.1007/s00125-019-4859-4>.
- [28] F. Lin, C. Song, Y. Zeng, Y. Li, H. Li, B. Liu, M. Dai, P. Pan, Canagliflozin alleviates LPS-induced acute lung injury by modulating alveolar macrophage polarization, *Int. Immunopharmacol.* 88 (2020) 106969.
- [29] M.E. Abdelmageed, R.S. Abdelrahman, Canagliflozin attenuates thioacetamide-induced liver injury through modulation of HMGB1/RAGE/TLR4 signaling pathways, *Life Sci.* 322 (2023) 121654, <https://doi.org/10.1016/j.lfs.2023.121654>.
- [30] Y. Niu, Y. Zhang, W. Zhang, J. Lu, Y. Chen, W. Hao, J. Zhou, L. Wang, W. Xie, Canagliflozin ameliorates NLRP3 inflammasome-mediated inflammation through inhibiting NF-κB signaling and upregulating Bif-1, *Front. Pharmacol.* 13 (2022) 820541.
- [31] W.A. Hewedy, S.A. Abdulmalek, D.A. Ghareeb, E.S. Habiba, AMPK-mediated autophagy is involved in the protective effect of canagliflozin in the vitamin D3 plus nicotine calcification model in rats, *Naunyn-Schmiedeberg Arch. Pharmacol.* (2023), <https://doi.org/10.1007/s00210-023-02627-x>.
- [32] M.M. Nakhel, P. Jayaprakash, S. Aburuz, B. Sadek, A. Akour, Canagliflozin Ameliorates Oxidative Stress and Aesthetic-like Features in Valproic-Acid-Induced Autism in Rats: Comparison with Aripiprazole Action, *Pharmaceuticals* 16 (5) (2023) 769.
- [33] L.H. Khedr, R.M. Eladawy, N.N. Nassar, M.A. Saad, Canagliflozin attenuates chronic unpredictable mild stress induced neuroinflammation via modulating AMPK/mTOR autophagic signaling, *J. Neuropharmacology* 223 (2023) 109293.
- [34] A. Sirichoat, S. Kruttsri, K. Suwannakot, A. Arananrochana, P. Chaisawang, W. Pannangrong, P. Wigmore, J.U. Welbat, Melatonin protects against methotrexate-induced memory deficit and hippocampal neurogenesis impairment in a rat model, *Biochem. Pharmacol.* 163 (2019) 225–233, <https://doi.org/10.1016/j.bcp.2019.02.010>.
- [35] S. Naewla, A. Sirichoat, W. Pannangrong, P. Chaisawang, P. Wigmore, J.U. Welbat, Hesperidin Alleviates Methotrexate-Induced Memory Deficits via Hippocampal Neurogenesis in Adult Rats, *Nutrients* 11 (4) (2019), <https://doi.org/10.3390/nu11040936>.
- [36] N. Sritawan, R. Prajit, P. Chaisawang, A. Sirichoat, W. Pannangrong, P. Wigmore, J.U. Welbat, Metformin alleviates memory and hippocampal neurogenesis decline induced by methotrexate chemotherapy in a rat model, *Biomed. Pharmacother.* 131 (2020) 110651, <https://doi.org/10.1016/j.biopha.2020.110651>.
- [37] M. Antunes, G. Biala, The novel object recognition memory: neurobiology, test procedure, and its modifications, *Cogn. Process.* 13 (2) (2012) 93–110, <https://doi.org/10.1007/s10339-011-0430-z>.
- [38] N.J. Broadbent, L.R. Squire, R.E. Clark, Spatial memory, recognition memory, and the hippocampus, *Proc. Natl. Acad. Sci.* 101 (40) (2004) 14515–14520, <https://doi.org/10.1073/pnas.0406344101>.
- [39] T.V. Gehring, G. Luksys, C. Sandi, E. Vasilaki, Detailed classification of swimming paths in the Morris Water Maze: multiple strategies within one trial, *Sci. Rep.* 5 (1) (2015) 14562, <https://doi.org/10.1038/srep14562>.
- [40] M.M. Bradford, A rapid and sensitive method for the quantitation of microgram quantities of protein utilizing the principle of protein-dye binding, *Anal. Biochem.* 72 (1–2) (1976) 248–254.
- [41] C.F.A. Culling, Handbook of histopathological and histochemical techniques: including museum techniques, Butterworth-Heinemann, 2013.
- [42] H. Abbas, H.A. Gad, M.A. Khattab, M. Mansour, The Tragedy of Alzheimer's Disease: Towards Better Management via Resveratrol-Loaded Oral Bilosomes, *Pharmaceutics* 13 (10) (2021), <https://doi.org/10.3390/pharmaceutics13101635>.
- [43] M.A. Thomaz, S.C. Acedo, C.C. de Oliveira, J.A. Pereira, D.G. Priolli, M.J. Saad, J. Pedrazzoli Jr, A. Gambero, Methotrexate is effective in reactivated colitis and reduces inflammatory alterations in mesenteric adipose tissue during intestinal inflammation, *J. Pharmacol. Res.* 60 (4) (2009) 341–346.
- [44] X. Li, R.P. Kerindongo, B. Preckel, J.-O. Kalina, M.W. Hollmann, C.J. Zuurbier, N. C. Weber, Canagliflozin inhibits inflammasome activation in diabetic endothelial cells—Revealing a novel calcium-dependent anti-inflammatory effect of canagliflozin on human diabetic endothelial cells, *J. Biomed. Pharmacother.* 159 (2023) 114228.
- [45] L.H. Khedr, N.N. Nassar, L. Rashed, E.D. El-denshary, A.M. Abdel-tawab, TLR4 signaling modulation of PGC1-α mediated mitochondrial biogenesis in the LPS-Chronic mild stress model: Effect of fluoxetine and pentoxifylline, *Life Sci.* 239 (2019) 116869, <https://doi.org/10.1016/j.lfs.2019.116869>.
- [46] S.D. Jayasingam, M. Citartan, T.H. Thang, A.A. Mat Zin, K.C. Ang, E.S. Ch'ng, Evaluating the Polarization of Tumor-Associated Macrophages Into M1 and M2 Phenotypes in Human Cancer Tissue: Technicalities and Challenges in Routine Clinical Practice, *Front. Oncol.* 9 (2020).
- [47] S. Zhang, C. Chu, Z. Wu, F. Liu, J. Xie, Y. Yang, H. Qiu, IFI1H Contributes to M1 Macrophage Polarization in ARDS, *Front. Immunol.* 11 (2020) 580838, <https://doi.org/10.3389/fimmu.2020.580838>.
- [48] F. Zhang, H. Wang, X. Wang, G. Jiang, H. Liu, G. Zhang, H. Wang, R. Fang, X. Bu, S. Cai, J. Du, TGF-β induces M2-like macrophage polarization via SNAIL-mediated suppression of a pro-inflammatory phenotype, *Oncotarget* 7 (32) (2016) 52294–52306, <https://doi.org/10.18632/oncotarget.10561>.
- [49] J. Chen, Z.-B. Huang, C.-J. Liao, X.-W. Hu, S.-L. Li, M. Qi, X.-G. Fan, Y. Huang, LncRNA TP73-AS1/miR-539/MMP-8 axis modulates M2 macrophage polarization in hepatocellular carcinoma via TGF-β1 signaling, *Cell. Signal.* 75 (2020) 109738, <https://doi.org/10.1016/j.cellsig.2020.109738>.
- [50] K. Yao, H.-b. Zu, Microglial polarization: novel therapeutic mechanism against Alzheimer's disease, *Inflammopharmacology* 28 (1) (2020) 95–110, <https://doi.org/10.1007/s10787-019-00613-5>.
- [51] S. Guo, H. Wang, Y. Yin, Microglia Polarization From M1 to M2 in Neurodegenerative Diseases, *Frontiers in Aging, Neuroscience* 14 (2022).
- [52] M. Liu, X. Meng, Z. Xuan, S. Chen, J. Wang, Z. Chen, J. Wang, X. Jia, Effect of Er Miao San on peritoneal macrophage polarisation through the miRNA-33/NLRP3 signalling pathway in a rat model of adjuvant arthritis, *Pharm. Biol.* 60 (1) (2022) 846–853, <https://doi.org/10.1080/13880209.2022.2066700>.



- [53] H.L. Lu, X.Y. Huang, Y.F. Luo, W.P. Tan, P.F. Chen, Y.B. Guo, Activation of M1 macrophages plays a critical role in the initiation of acute lung injury, *Biosci. Rep.* 38 (2) (2018), <https://doi.org/10.1042/bsr20171555>.
- [54] R. Hasan, S. Lasker, A. Hasan, F. Zerin, M. Zamila, F.I. Chowdhury, S.I. Nayan, M. M. Rahman, F. Khan, N. Subhan, M.A. Alam, Canagliflozin attenuates isoprenaline-induced cardiac oxidative stress by stimulating multiple antioxidant and anti-inflammatory signaling pathways, *Sci. Rep.* 10 (1) (2020) 14459, <https://doi.org/10.1038/s41598-020-71449-1>.
- [55] O. Butovsky, M.P. Jedrychowski, C.S. Moore, R. Cialic, A.J. Lanser, G. Gabriely, T. Koeglspberger, B. Dake, P.M. Wu, C.E. Doykan, Z. Fanek, L. Liu, Z. Chen, J. D. Rothstein, R.M. Ransohoff, S.P. Gygi, J.P. Antel, H.L. Weiner, Identification of a unique TGF- $\beta$ -dependent molecular and functional signature in microglia, *Nat. Neurosci.* 17 (1) (2014) 131–143, <https://doi.org/10.1038/nn.3599>.
- [56] J. Zhang, H. Jiang, F. Wu, X. Chi, Y. Pang, H. Jin, Y. Sun, S. Zhang, Neuroprotective Effects of Hesperetin in Regulating Microglia Polarization after Ischemic Stroke by Inhibiting TLR4/NF- $\kappa$ B Pathway, *J. Healthcare Eng.* 2021 (2021) 9938874, <https://doi.org/10.1155/2021/9938874>.
- [57] F. Safaei, S. Mehrzadi, H. Khadem Haghighian, A. Hosseinzadeh, A. Nesari, M. Dolatshahi, M. Esmailizadeh, M. Goudarzi, Protective effects of gallic acid against methotrexate-induced toxicity in rats, *Acta Chir. Belg.* 118 (3) (2018) 152–160, <https://doi.org/10.1080/00015458.2017.1394672>.
- [58] M. Roghani, H. Kalantari, M.J. Khodayar, L. Khorsandi, M. Kalantar, M. Goudarzi, H. Kalantar, Alleviation of Liver Dysfunction, Oxidative Stress and Inflammation Underlies the Protective Effect of Ferulic Acid in Methotrexate-Induced Hepatotoxicity. *Drug Des., Develop. Ther.* 14(null) (2020) 1933–1941. doi: 10.2147/DDDT.S237107.
- [59] A.Y. Al-Taher, M.A. Morsy, R.A. Rifaai, N.M. Zenhom, S.A. Abdel-Gaber, Paeonol Attenuates Methotrexate-Induced Cardiac Toxicity in Rats by Inhibiting Oxidative Stress and Suppressing TLR4-Induced NF- $\kappa$ B Inflammatory Pathway, *Mediators Inflamm.* 2020 (2020) 8641026, <https://doi.org/10.1155/2020/8641026>.
- [60] R.G. Baker, M.S. Hayden, S. Ghosh, NF- $\kappa$ B, inflammation, and metabolic disease, *Cell Metab.* 13 (1) (2011) 11–22.
- [61] Y.-f. Li, G. Nanayakkara, Y. Sun, X. Li, L. Wang, R. Cueto, Y. Shao, H. Fu, C. Johnson, J. Cheng, X. Chen, W. Hu, J. Yu, E.T. Choi, H. Wang, X.-f. Yang, Analyses of caspase-1-regulated transcriptomes in various tissues lead to identification of novel IL-1 $\beta$ , IL-18- and sirtuin-1-independent pathways, *J. Hematol. Oncol.* 10 (1) (2017) 40, <https://doi.org/10.1186/s13045-017-0406-2>.
- [62] L. Xiao, H. Zheng, J. Li, Q. Wang, H. Sun, Neuroinflammation Mediated by NLRP3 Inflammasome After Intracerebral Hemorrhage and Potential Therapeutic Targets, *Mol. Neurobiol.* 57 (12) (2020) 5130–5149, <https://doi.org/10.1007/s12035-020-02082-2>.
- [63] C.J. Zuurbier, NLRP3 Inflammasome in Cardioprotective Signaling, *J. Cardiovasc. Pharmacol.* 74 (4) (2019).
- [64] J. Sai, L. Xiong, J. Zheng, C. Liu, Y. Lu, G. Wang, Y. Wang, T. Wang, X. Guan, F. Chen, K. Fang, C. Zhang, J. Lu, X. Zhang, H. Zhu, F. Wang, Protective Effect of Yinhuo Miyanling Tablet on Lipopolysaccharide-Induced Inflammation through Suppression of NLRP3/Caspase-1 Inflammasome in Human Peripheral Blood Mononuclear Cells, *Evid. Based Complement. Alternat. Med.* 2016 (2016) 2758140, <https://doi.org/10.1155/2016/2758140>.
- [65] Y. Hong, Y. Liu, D. Yu, M. Wang, Y. Hou, The neuroprotection of progesterone against A $\beta$ -induced NLRP3-Caspase-1 inflammasome activation via enhancing autophagy in astrocytes, *Int. Immunopharmacol.* 74 (2019) 105669, <https://doi.org/10.1016/j.intimp.2019.05.054>.
- [66] R. Aryanpour, P. Pasbakhsh, K. Zibara, Z. Namjoo, F. Beigi Boroujeni, S. Shahbeigi, I.R. Kashani, C. Beyer, A. Zendehele, Progesterone therapy induces an M1 to M2 switch in microglia phenotype and suppresses NLRP3 inflammasome in a cuprizone-induced demyelination mouse model, *Int. Immunopharmacol.* 51 (2017) 131–139, <https://doi.org/10.1016/j.intimp.2017.08.007>.
- [67] E.H.M. Hassanein, F.M. Saleh, F.E.M. Ali, E.K. Rashwan, A.M. Atwa, O.A.M. Abd El-Ghafar, Neuroprotective effect of canagliflozin against cisplatin-induced cerebral cortex injury is mediated by regulation of HO-1/PPAR- $\gamma$ , SIRT1/FOXO-3, JNK/AP-1, TLR4/iNOS, and Ang II/Ang 1–7 signals, *Immunopharmacol. Immunotoxicol.* 45 (3) (2023) 304–316, <https://doi.org/10.1080/08923973.2022.2143371>.